

EMISSIVITY OF HIGH TEMPERATURE AIR

James Keck, Bennett Kivel, Tunis Wentink, Jr.
Avco Research Laboratory, Everett 49, Mass.

1. INTRODUCTION

The absolute emissivity of high temperature air (4000 to 9000°K at normal density) has received little attention until recently. * Hirschfelder and Magee** touch on this "low temperature" region. For rough estimates they consider only the free-free absorption of O⁻ and N⁻ but mention the O⁻ photoelectric effect and NO₂ absorptions. At the other extreme measurements have been made on cold air***
****. With the advent of the shock tube and high speed spectroscopy measurements in the intermediate range are now possible.

The present report summarizes the progress of our studies to date. While we are still far from a complete understanding of all the processes involved in producing radiation from air, we have gained considerable insight to the problem and have accumulated data which we believe give reasonable estimates of the emissivity.

Perhaps the major result of the work completed to date is the realization that NO appears to contribute considerably less to the radiation from air than was estimated assuming typical values for the unknown transition probability of this molecule but that the emissivity is not therefore negligible. The problem has in fact taken on a new complexity due to the necessity of considering a number of other species which now contribute comparable intensities.

2. PREDICTION OF EMISSIVITY2.1 Emissivity of High Temperature Air

Without knowledge of absolute transition probabilities predictions are difficult. Preliminary unpublished studies by H. Bethe, H. Mayer and R. Meyerott indicated that the NO β and γ bands would give the most radiation energy if their f number was like 0.1. The measurements indicate that this is not the case and that several radiating species must be considered.

The pertinent information to be analyzed are: 1) the spectrum of air at 8000°K and .85 normal density, 2) the absolute spectral emissivity of a plane optically thin layer of air at 8000°K and .85 normal density and 3) the spectral emissivity of a thin layer of air at .85 normal density for various wavelengths as a function of temperature in the range 5000°K to 9000°K.

-
- * R. Meyerott of Rand Corporation is currently making a survey of all pertinent phenomena.
- ** J. O. Hirschfelder and J. L. Magee, Opacity and Thermodynamic Properties of Air at High Temperatures, Los Alamos Declassified Report (LADC) 943, July 18, 1945.
- *** E. G. Schneider, J. O. S. A. 30, 128 (1940).
- **** K. Watanabe, M. Zelikoff and E. C. Y. Inn, Absorption Coefficients of Several Atmospheric Gases. (G. R. D. - A. R. D. C., Cambridge, June 1953).
R. W. Ditchburn, Proc. Roy. Soc. Lond, 236, 216 (1956).

Our procedure will be to assume thermodynamic equilibrium and nominate six likely systems as the main radiators. In order of increasing wavelength they are: 1) the β and γ bands of NO, 2) the second positive bands of N_2 , 3) the CN violet bands, 4) the free-bound transitions forming O^- , 5) the first positive bands of N_2 and 6) the free-free transitions of electrons scattered by O. Of these systems positive spectroscopic identification has been obtained only for CN and the first and second positive band systems of N_2 . For the continua theoretical considerations given in Section 4 coupled with general features of the spectral emissivity and its variation with temperature make the other choices very plausible. Since the CN radiation and the free-bound and free-free radiation associated with O can be estimated on the basis of other data, the theory has as free parameters only the unknown f numbers for the bands of NO and N_2 . These have been adjusted to fit the spectral emissivity in appropriate regions of the spectrum. In Fig. 1 the theoretical curve so derived is compared with the experimental results it was adjusted to fit. The general agreement is not surprising in view of the three adjustable parameters in the theory. The disagreement in the CN region could easily be due to excess CO_2 in the air of an industrial locality and is not considered significant.

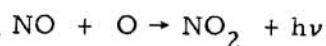
Table 1 lists the six systems considered with appropriate f numbers and their contribution to the total emissivity at $8000^\circ K$ and .85 atmospheric density. The difference between the experimental and theoretical values for the total emissivities is due to the fact that we have not adjusted the radiation associated with O to fit our data but calculated it on an absolute basis as described in Section 4.4. While the discrepancy is probably well within the uncertainty of the theory, the possibility also exists that the additional radiation could be due to an excess electron concentration in the shock tube due to ionized impurities. It is important to note that the f number for NO is considerably less than 0.1.

Table 1

Emissivity of optically thin air attributed to six radiating species. The f numbers except for CN are deduced from absolute emissivities at appropriate wavelengths. They are subject to the assumption that the large number of lines in the molecular bands can be treated as a continuum. They are defined as the f numbers per initial electronic state.

Source	f number	% emissivity cm^{-1} ϵ/L
NO (β and γ) ($.2\mu < \lambda$)	.0025	1.1
N_2 (2 nd. pos.)	.07	1.1
CN (violet)	.1	.1
O^- (free-bound)		.4
N_2 (1st. pos.) ($\lambda < 1\mu$)	.02	.6
O + e (free-free) ($\lambda < 1\mu$)		.1
Total Theoretical Emissivity ($.2 < \lambda < 1\mu$)		<u>3.4</u>
Total Experimental Emissivity ($.2 < \lambda < 1\mu$)		3.5

A number of obvious systems have been omitted in the list given above because their contributions are expected to be negligible. Among them are the recombination radiation from the processes



and



which should be studied more carefully. The CN red bands, O₂ Schumann-Runge and N₂⁺ first negative bands, also omitted, are not necessarily negligible.

Measurements of the Mach number dependence of the radiation at a number of wavelengths have been made using the monochromator and photocells. The results are compared with theoretical predictions in Fig. 2. The wavelengths were chosen to emphasize the radiation from each of the major contributors. The relative ordinates of the various curves is not significant as they have been arbitrarily displaced to avoid overlapping. Agreement between the theory and experiment is very satisfactory and can be regarded as confirmation of the predicted temperature dependence of the radiation as the dependence on density is relatively very weak.

2.2 Relation of Emissivity to Absorption Coefficient.

In order to relate the measured emissivity to the absorption coefficient, we consider the radiation from a plane parallel gas. For generality we consider the surface of our detector to be reflecting. Then the flux is given by:

$$F = \int_0^\infty \pi \epsilon_\lambda B_\lambda (1 - r_\lambda) d\lambda \quad (1)$$

where B_λ is the Planck distribution:

$$B_\lambda = \frac{2hc^2/\lambda^5}{(e^u - 1)}, \quad u = hc/\lambda kT; \quad (2)$$

ϵ_λ is the spectral emissivity of the air and r_λ is the spectral reflectance of the wall. And

$$\epsilon_\lambda \doteq (1 - e^{-2\tau_\lambda}), \quad (3)$$

where

$$\tau_\lambda = \int_0^L \mu'_\lambda dz, \quad (4)$$

and

$$\mu' = \mu(1 - e^{-u}); \quad (5)$$

μ is the absorption coefficient and L is the thickness of the radiating layer. Since the experiments show that the emissivity is small for the range of conditions of interest, we may use an approximation to Eq. (3) which is valid for optically thin layers at uniform temperature:

$$\epsilon_\lambda \doteq 2\mu' L, \quad \epsilon_\lambda \ll 1, \quad (6)$$

If the radiation is due to a number of sources, then in the approximation of Eq. (6) we can express ϵ_λ as a sum over the emissivities of the individual sources, :

$$\epsilon_\lambda = \sum_i \epsilon_{\lambda i}, \quad \epsilon_\lambda \ll 1 \quad (7)$$

Since in most practical cases the term $(1 - r_\lambda)$ does not vary rapidly over the spectral region giving the largest contribution from a single species a good approximation can be obtained by factoring $(1 - r_\lambda)$ out of the integral and replacing it by its mean value for the i th species. Eq. (1) then becomes:

$$F = \sum_i (1 - r_{\lambda i}) \int_0^\infty \pi \epsilon_{\lambda i} B_\lambda d\lambda, \quad \epsilon_\lambda \ll 1 \quad (8)$$

The integral in Eq. (8) is by definition just the black body flux σT^4 times the total emissivity of the i th species, ϵ_i . We can therefore write Eq. (8) in a form convenient for calculations:

$$F = \sigma T^4 \sum_i (1 - r_{\lambda})_i \epsilon_i, \quad \epsilon_{\lambda} \ll 1 \quad (9)$$

The wavelength at which $(1 - r_{\lambda})$ is to be evaluated can be determined by inspection of Fig. 1 which gives the approximate spectral distribution for the various species. ϵ_i can be determined as a function of temperature, density and thickness of the radiating layer using the equilibrium composition of air*.

For purposes of estimating the radiative flux from hot air we set the reflectivity in Eq. (9) equal to zero. We are then left with the particularly simple result:

$$F = \epsilon \sigma T^4 \quad r_{\lambda} = 0, \quad \epsilon_{\lambda} \ll 1 \quad (10)$$

where

$$\epsilon = \sum_i \epsilon_i \quad (11)$$

This sum Eq. (11) has been evaluated for a 1 cm layer of air and is plotted as a function of T and ρ/ρ_0 in Fig. 3.

3. EMISSION OF AIR: EXPERIMENTAL

3.1 Radiation Source

In all of the experiments described below the source of the radiation studied was dry air heated by a shock wave reflected from the end of a closed shock tube. This technique** has been used previously by workers at Cornell to study the radiation from high temperature Argon***.

Observations were made through a quartz window in the end of the tube. Since the temperature and density behind the incident shock are relatively low, little radiation is observed prior to reflection of the incident shock at the end of the tube. Subsequent to reflection the hot air layer behind the reflected shock becomes highly luminous. Observations may be made on this layer, which grows at a constant rate of $\sim .07$ cm./ μ s, for an interval of $\sim 30 \mu$ s. At this time the mixed region ahead of the contact discontinuity encounters the reflected shock and effectively terminates the "good seeing" by introducing dust and foreign gases into the heated region. The temperature and density behind the reflected shock and the reflected shock velocity were calculated by applying the laws of conservation of mass, momentum, and energy and assuming full thermodynamic equilibrium. This assumption, which is important in many aspects of this type of research, received considerable theoretical and experimental attention and, although the results are probably not definitive, the general feeling is that equilibrium is achieved in a few microseconds in the high temperature range of interest here. If this is the case, then the conditions behind the reflected shock will be uniform (neglecting attenuation) and the radiation can be expected to increase linearly with time if the emissivities are small. This is actually observed and provides additional evidence that the equilibrium assumption is valid.

Since considerable radiation occurs after the driver gases encounter the

* F.R. Gilmore, Rand Corporation Research Memorandum, RM-1543 (1955).

** E. L. Resler, S.C. Lin, and A. Kantrowitz, J. Appl. Phys. 23, 1390 (1952).

*** H.E. Petschek, P.H. Rose, H.S. Glick, A. Kane, and A. Kantrowitz, J. Appl. Phys. 26, 83 (1955).

reflected shock, all observations must be made on a time resolved basis. Data obtained to date include:

- (a) Time resolved spectrograms.
- (b) Absolute intensity measurements made with a calibrated monochromator and photocells.

The wave length region investigated in detail extends from approximately 2500\AA to 9000\AA . In the following sections details of the experimental work completed are presented.

3.2 Spectra: Experimental

The spectroscopic portion of the radiation program was devoted largely to the identification and measurement of relative intensities of radiating species.

Time-resolved emission spectra (resolution about $10\text{ }\mu\text{sec.}$) were obtained using a spectrograph equipped with a drum camera. The instrument, shown in Fig. 4, is a Hilger Medium Quartz Prism Spectrograph (characteristics similar to Hilger Type E 498, optical speed about $f/10$) modified to record the data with a drum camera. The drum, pneumatically driven, was operated at linear speeds of 32 to 128 meters/second, resulting in time dispersion of 31 to 8 microseconds/millimeter. The instantaneous slit image on the film was approximately 1 mm high. Slit widths ranging from 30 to 250 microns were used. The larger widths were necessary in exploring the photographic infrared region. The spectral dispersion characteristic is typical of a medium size quartz prism, and may be judged by the wavelength scales of the accompanying figures.

The spectral range of the original instrument was about 2000 to $10,000\text{\AA}$. However, several factors restricted the useable range after modification to approximately 2500 to 8800\AA . The short wavelength sensitivity limit is dictated by the optical train, the long wavelength cut-off is governed by film emulsion sensitization.

The spectra are presented and discussed below. The overall results are that in shock tube air at 8000°K and in the spectral region studied, ($2500\text{--}8800\text{\AA}$) the major detected species are N_2 and CN. The NO band spectrum is too smeared at 8000°K to be easily identified.

Ultraviolet Region

Figs. 5 and 6 show the spectra and corresponding densitometer curves for air at wavelengths below 4000\AA . It is in this region, and especially below 3000\AA that the NO β -band system is expected to have appreciable intensity. The predicted spectral distribution is given in Fig. 1*. No positive identification of any NO bands has been made in any of our spectra. In those runs in which NO was intentionally introduced into the shock tube, or in higher density runs (5 cm) in air in which the NO concentration would be expected to be greater than in the usual 1 cm. experiments, only bands characteristic of N_2 and CN were found.

However, a definite band system has been observed which must be assigned as the Second Positive System in N_2 (See Fig. 5 and 6). The spectral distribution is in good agreement with that predicted theoretically at 8000°K . The presence of N_2 Second Positive indicates that the First Positive System of N_2 can also be expected;

* B. Kivel, H. Mayer and H. Bethe, Emissivity of Nitric Oxide in High Temperature Air. To be published.

this system has been tentatively observed and is discussed later in connection with the red region.

Visible and Photographic Near-Infrared Region

The observed radiation in the ultraviolet and blue (up to about 4400\AA) has been attributed to N_2 and CN. Above 4400\AA the radiation shows little structure. This radiation may be due to the reaction $\text{O} + \text{electron} \rightarrow \text{O}^+ + h\nu$ discussed elsewhere in this report. Further study of this region is desirable, since the continuous distribution makes identification difficult. We have begun examination of this region using O_2 -Argon mixtures to investigate this suspected O^+ continuum but no results are yet available. The spectrum is shown in Fig. 7.

In the red and near-infrared the results must be considered preliminary due to the marginal sensitivity and resolution. The resolution is particularly poor in the near-infrared, due to the characteristics of the I-N film and the wide slits necessary to obtain useful intensities. However, the radiation above 5500\AA can best be ascribed to the First Positive System of nitrogen. In Fig. 7 the theoretical intensity distribution for Nitrogen First Positive in air at 8000°K has been plotted on the raw densitometer data. In this theoretical curve the intensity is that expected if a "flat" and linear detector were used; i. e., there has been no correction for the spectral sensitivity or spectrograph dispersion. The agreement is such that the First Positive System of N_2 can be reasonably safely assigned.

The interference due to the potassium (K) doublet in the "wrap around" can also be seen. The presence of this internal calibration standard, however, has allowed tentative identification of the atomic oxygen line at 7772\AA . This line is visible in shock spectra in air under experimental conditions when Nitrogen First Positive is not observed (e. g. narrow slits or weak ($M = 11$) shocks). At higher temperatures ($M = 13$) and with wider slits the atomic O line blends into the more complicated nitrogen band system. It is of interest to consider the energies involved in the various observed transitions. The upper levels which give rise to the CN violet and CN red band systems are, respectively, at 3.22 and 1.36 volts above the ground vibrational state in CN. As expected, these levels are readily excited in shock spectra.

The transitions leading to the Second Positive Group in molecular nitrogen involve levels from 11.05 ev. (89150 cm^{-1}) down to 7.39 ev. (59625 cm^{-1}) all relative to the ground vibrational state for N_2 . The First Positive Group in turn results from transitions between levels at 7.39 ev. (59625 cm^{-1}) down to 6.22 ev. (50200 cm^{-1}).

The γ bands of NO arise from upper levels at 5.45 ev. (43960 cm^{-1}). Since these levels should be readily excited at the temperatures in question, the lack of NO bands in our spectra can be attributed in part to the low f -number deduced from our other experiments but mostly to the vibration and rotation smearing at 8000°K .

The atomic oxygen line at 7772\AA results from a transition from 10.74 ev. (86625 cm^{-1}) to 9.15 ev. (73768 cm^{-1}) above the atomic oxygen ground state, which in turn is 5.11 ev. above the molecular oxygen ground vibrational state. Hence levels 15.85 ev. above the molecular ground state of O_2 are excited to a measurable extent in air at 8000°K . It is of interest to note that Whipple has informed us that he has observed emission from meteors characteristic of N_2 (Second Positive) and atomic oxygen.

3.3 Monochromator-Photocell Measurements

A measurement of the spectral emissivity of high temperature air has been made in the wavelength range from 2300\AA to 9500\AA using a monochromator and

photocells. Measurements in the red were made using an RCA 917 phototube while those in the violet were made using an RCA 935 phototube. The rise time of the electronics associated with the phototubes was $.3 \mu\text{sec}$. Absolute intensity calibrations were carried out using a tungsten ribbon filament lamp and the crater of a carbon arc as standards. The true temperatures of these sources determined with a Leeds and Northrup optical pyrometer were respectively 2765°K and 3970°K . Data on the emissivity of tungsten was taken from the Smithsonian Physical Tables; the arc was assumed to be a gray body with an emissivity of .85. From 4000\AA to 10000\AA the two calibrations agreed within 10%. Below 4000\AA only the carbon arc could be used due to the cut-off of the glass envelope of the lamp and we are therefore somewhat less certain of the calibration in this range. The optics for calibration were identical to those used in the shock tube runs so that intensities were obtained directly as ratios to the intensity of the standard and no geometrical or absorption correction were necessary.

For these initial measurements of the spectral distribution of the radiation from air the initial pressure, P_1 , in the shock tube was 1 cm of Hg and the shock Mach number was $13.2 \pm .5$. This gave a temperature and density behind the reflected shock of $8050 \pm 200^\circ\text{K}$ and $.85 \pm .03$ normal. The errors indicated are not the uncertainties in measurements but rather give the maximum dispersion in values associated with fluctuations in the Mach number from run to run. In principle it would have been possible to make a first order correction for such fluctuations but this was not done due to a failure to detect a significant correlation between output signal and Mach number. Unfortunately, due to the limited data obtained to date we do not have a sufficient sample at any one point to give an estimate of the reproducibility of the points. However, our best guess based on inspection of Fig. 1 is that the results are reproducible to $\pm 10\%$.

A typical set of oscillograms of the phototube output is shown in Fig. 8. The traces are observed to rise linearly for the experimental time of $\sim 30 \mu\text{sec}$. This was characteristic of all spectral regions investigated and implies that the radiation is proportional to thickness and, hence, that the spectral emissivities are small compared to unity. It may also be taken as evidence that the layer behind the reflected shock is in thermal equilibrium. The argument here is that if a chemical species capable of radiating appreciably were being formed at a constant rate it would add a quadratic term to the time dependence of the intensity.

The measured wavelength dependence of the radiation from a 1 cm layer of air at a temperature of 8050°K and .85 normal density is plotted in Fig. 1 and tabulated in Table 2. The first column in Table 2 gives the mean wavelength, $\bar{\lambda}$, for an interval and the second column gives the wavelength, λ , separating intervals. The third column gives the mean spectral steradiancy, $I_{\bar{\lambda}}$. The fourth column gives the integral steradiancy, I , defined by the expression:

$$I = \int_{.22\mu}^{\lambda} I_{\bar{\lambda}} d\lambda \quad (12)$$

The last column gives the spectral emissivity per cm. $\epsilon_{\bar{\lambda}}/L$ defined by the expression:

$$\epsilon_{\bar{\lambda}}/L = 2 I_{\bar{\lambda}}/B_{\bar{\lambda}} \quad (13)$$

where $B_{\bar{\lambda}}$ is given by Eq. (2).

The Mach number dependence of the radiation is shown in Fig. 2. The initial pressure was kept fixed at 1 cm. of Hg. with the result that both temperature and density varied behind the reflected shock as shown by the supplementary scales on the abscissa. The intensity measurements are relative and the order of the curves

Table 2

Spectral Sterradiance, $I_{\bar{\lambda}}$, Integral Sterradiance, $\int_{.22}^{\lambda} I_{\bar{\lambda}} d\lambda$, and Spectral Emissivity, $\epsilon_{\bar{\lambda}}/L$, of 1 cm. of Air at 8050°K and .85 Normal Density.

B_{λ} is the Planck Distribution for a Black Body at 8000°K.

$\bar{\lambda}$	λ	$I_{\bar{\lambda}}$	$\int_{.22}^{\lambda} I_{\bar{\lambda}} d\lambda$	B_{λ}	$\epsilon_{\bar{\lambda}}/L$
μ	μ	w/cm ³ ster	w/cm ³ ster	w/cm ² ster	cm ⁻¹
.23	.24	540	11	7500	.145
.25	.26	360	18	9300	.078
.27	.28	380	26	10700	.071
.29	.30	440	34	12000	.074
.31	.32	500	44	12900	.077
.33	.34	410	53	13300	.062
.35	.36	360	60	13600	.053
.37	.38	340	67	13600	.050
.39	.40	430	75	13400	.064
.4125	.425	180	80	13000	.028
.45	.475	115	86	12100	.018
.50	.525	105	91	10800	.020
.55	.575	80	94	9400	.017
.60	.625	84	99	8000	.021
.65	.675	123	105	6900	.036
.70	.725	109	110	5900	.037
.75	.775	78	114	5000	.031
.80	.825	62	118	4300	.029
.85	.875	64	121	3750	.034
.90	.925	45	123	3150	.029
.95	.975	64	127	2750	.047

corresponding to different wavelength settings on the monochromator is arbitrary. The crosses and circles are used to aid in the separation of the different curves. The wavelengths were chosen to emphasize the radiation from various species as indicated. Since the variation in density is slight, and the dependence on the parameter is weak, the curves may be regarded as giving essentially the temperature dependence of the radiation.

The agreement between theory and experiment is very good. However, it cannot be regarded as establishing the fundamental correctness of the theory, since it can be seen that the temperature dependence is not very sensitive to a particular species. This is, of course, to some extent accidental but it is indicative of the situation.

Measurements of the density dependence of the radiation are currently in progress and although the results have not been analyzed in detail, there is no indication of any serious discrepancies arising.

4. THEORETICAL STUDIES

The absorption coefficient of air as a function of frequency, temperature and density cannot be obtained by theoretical means alone. Even with high speed computing machines reliable estimates of the electronic (absolute) transition probabilities for molecular band systems cannot be obtained. However, the theory does

give relative values and can be used to search out inconsistencies in the experiments and to extend the measurements to other temperatures and densities.

Before any measurements were made, attention was centered on a most likely source: - the $\text{NO}\beta$ and γ bands. The measurements described above indicate that this system is not dominant and many other species contribute. Most of the radiators of interest are being studied theoretically by R. Meyerott of the Rand Corporation. At Avco we have made detailed calculations for the $\text{NO}\beta$ and γ system (H. Bethe, H. Mayer and B. Kivel, to be published elsewhere). More recently we have made rough calculations for the N_2 first positive band system, CN violet band system, N_2 second positive band system, O^- bound-free and $\text{O} + e$ Bremsstrahlung. In all of this work the equilibrium composition of air obtained by F.R. Gilmore of Rand Corporation has been an important aid.*

The work of H. Bethe and H. Mayer on NO are too elaborate to present here and it is hoped that this material will be given in a separate publication. The work is similar to our treatment of N_2 below but, in more detail. Of course, the absolute f numbers are not known and for purpose of the present analysis we assume it is the same for β and γ system.

The N_2 first positive system calculation is of the same type but slightly less accurate. A particular approximation which remains to be checked is the effect of spectral line width. In our work we have assumed the lines to be sufficiently broad so that the bands form a continuum. For predicting emissivities, this is not serious but should be remembered when quoting the f numbers. Perhaps our experimentally determined values are better called "effective f" numbers, because if the lines are too thin, then the actual f number is larger than given by our experiments.

A summary of the most recent theoretical calculations are presented here.

4.1 The CN Violet Band System

In the preliminary spectra of air obtained in the Avco shock tubes the CN violet bands are prominently displayed. It has been assumed that this is at least partly a result of carbon containing impurities in the air, especially, oil. It is interesting therefore to ask how intense is the CN spectra from equilibrium air of normal composition where the carbon comes only from CO_2 .

The vibration overlap integrals** for these transitions are available. The f number is also (comparatively speaking) well known***. For its value we take 0.1. Computed values of the overlap integrals for the more important bands are available from P.A. Fraser, W.R. Jarman and R.W. Nicholls, Report #10, Univ. of Western Ontario; wavelengths are from R.W.B. Pearse and A.G. Gaydon, Molecular Spectra, (J. Wiley & Sons, New York, 1950). The intensity near the vibration less transition ($v' = 0, v'' = 0$) band head at $\lambda = 3883\text{\AA}$ is .21 watts/cm² A for a 1 cm thick gas.

The emissivity for this system at $T = 8000^\circ\text{K}$, $\rho/\rho_0 = 1$, $L = 1\text{ cm}$ is estimated to be about 0.1% as follows. We have found $I \approx .2\text{ watts/cm}^2\text{ A}$ and the bands cover about 70 A. There are other bands which increase the emitted energy by less than a factor 2 bringing the total emission to about 30 watts/cm². However at 8000°K ,

* F.R. Gilmore, Rand Corporation Research Memorandum, RM-1543 (1955).

** P.A. Fraser, Proc. Phys. Soc. Lond. A67, 939 (1954).

*** A.G. Gaydon, Spectroscopy and Combustion Theory, (Chapman and Hall, London, (1948). p 143.

$$\sigma T^4 = 23 \text{ kilowatts/cm}^2.$$

4.2 The Nitrogen Second Positive Band System

Study of the air spectra obtained at the Avco Research Laboratory has revealed the presence of the nitrogen second positive band system.

The number of nitrogen molecules in the $B^3\Pi$ states with vibration quantum number v'' that can absorb these bands ($N_{N_2, B^3\Pi}$) is expressed for equilibrium in terms of the number of ground state N_2 molecules (N_{N_2}) by

$$N_{N_2, B^3\Pi} = 6e^{-(7.39/kT) - 0.215 v''/kT} \left(\frac{2.010}{1.638} \right) \left(\frac{0.292}{kT} \right) N_{N_2}$$

and

$$N_{N_2} = 5.3 \times 10^{19} \psi_{N_2} \rho/\rho_0$$

where ρ/ρ_0 is the density compared to normal air and F.R. Gilmore has given values of ψ_{N_2} . In obtaining this expression we have taken the electron degeneracy for the $B^3\Pi$ state to be 6 compared to 1 for the ground $X^1\Sigma$ state; the excitation energy in the $B^3\Pi$ state is approximately $7.394 + 0.215 v''$ e.v.; the smaller rotation constant results in a larger population of the excited state in the ratio $(B_{eX^1\Sigma}/B_{eB^3\Pi}) = (2.01/1.638)$; and the vibration partition function for the $X^1\Sigma$ state has been approximated by $(kT/hc \omega_{ex}) = (kT/0.292 \text{ ev})$.

We consider the 0,0 band which occurs at $\lambda = 3371\text{\AA}$ (3.678 ev) for $T = 8000^\circ\text{K}$, $\rho/\rho_0 = 1$, $L = 1 \text{ cm}$. First we note that

$$N_{N_2, B^3\Pi} = 6.8 \times 10^{-5} N_{N_2}$$

This population is on the order of the population of the N_2^+ ground state at this temperature and density. Thus if we see N_2 second positive we can also expect to see N_2^+ main system which absorbs from the ground state. Some of these bands have been found by John Camm of the Avco staff. Other molecules present in this concentration according to F.R. Gilmore are CO, NO, NO^+ , O_2 . The CO bands are in the ultraviolet and will not be observed; the NO^+ are not known - the Avco shock tube experiments may provide an opportunity for investigating this species. In O_2 there are the Schumann-Runge bands and in NO the β bands which one expects to find in the high energy end of the spectrum. In these systems the lower energy bands occur at larger internuclear separations, if the f value decreases with increasing internuclear separation then these bands may be hard to detect.

Taking the vibration overlap integral $q = .448$ and $f = .01$ the intensity per angstrom at the band head of the 0,0 transition in the nitrogen second positive system is .64 watts/cm² A for a 1 cm thick gas at $\rho/\rho_0 = 1$, $T = 8000^\circ\text{K}$.

For CN in normal air we get $I_{00} = .18 \text{ watts/cm}^2 \text{ A}$. However, the CN have I values greater than the N_2 in our spectrum implying either that the f value is considerably larger for CN, there is carbon impurity in the shock tube or both. It is also interesting to compare the intensity from an NO β band in this region; e.g. for $v' = 0 \rightarrow v'' = 11$ at $\lambda = 3804$ with $q = .1$ and $f = 0.1$, $I_{0,11} = .38 \text{ watts/cm}^2 \text{ A}$. This has the consequence that if the f value were .01 this band would be masked by the N_2 second positive bands. The $0 \rightarrow 5$ band occurs at $\lambda = 2754$; giving it a value $q = .1$ and $f = .1$ yields $I_{0,5} = 2.4 \text{ watts/cm}^2 \text{ A}$. Here again a decrease of a factor 10 in f number would account for the failure to observe this band.

We estimate the integrated emissivity as follows. We take the bands to

cover a 2000 Å region, and estimate that at $T = 8000^\circ\text{K}$, $\rho/\rho_0 = 1$ and $L = 1$ cm the intensity is about $1/4$ watt/cm² Å, then we get $1/2$ kilowatt/cm² or an emissivity of about 2%. This is on the same order of magnitude as predictions for the N_2 first positive system. Of course, quantitative comparison depends on the unknown factors.

There is an easy way to estimate the emissivity as a function of temperature and density. The most important temperature change is the decrease in the number of molecules in the excited $\text{B}^3\Pi$ state. Since the binding energy for this state is approximately 7.36 e.v., at temperatures below 8000°K the percent emissivity is given by $2 \exp [10.68 - 7.36/kT]$. Taking account of the slight increase of N_2 density with decreasing temperature we estimate:

$T (^\circ\text{K})$	8000	7000	6000	5000
$\epsilon (\%)$	2.	.43	.060	.0023

At the other extreme where the gas is optically thick the N_2 region becomes black and the emissivity is limited by the spectral region covered. If we take this region to extend from $\lambda = 2800\text{Å}$ to 3600Å then the maximum emissivity is:

$T (^\circ\text{K})$	8000	7000	6000	5000
$(\%)$	14.4	10.6	6.5	3.

4.3 Intensity Distribution for the N_2 First Positive Band System

In order to help in the identification of the N_2 First Positive Band System we have prepared a rough sketch of the expected emission appearance from a thin gas at 8000°K . This distribution was obtained using the overlap integrals given by Jarman, Nicholls and Turner*. (see Fig. 7)

4.4 O Bound-free and Free-free Radiators

In an ionized gas, radiation may occur due to collisions between free electrons and other gas particles. From a classical point of view, the collisions result in an acceleration of the electrons which produces radiation. In air, at about 8000°K , most of this radiation is probably due to collisions with oxygen atoms since these atoms can form negative ions indicating that a strong attractive field exists between the neutral atom and free electrons. This radiation may be subdivided into two components: 1) photo-recombination in which the free electron is captured into the bound state of O^- and 2) free-free radiation in which the electron remains free after the collision but has lost some kinetic energy.

Branscomb and Smith** have measured the cross-section for ionization of O^- as a function of wavelength by measuring the absorption of light in a mass spectrometer analyzed beam of O^- ions. Their results indicate a cross section which rises gradually from zero at an apparent threshold of 1.45 e.v. to about 10^{-17} cm² at a photon energy of 3 e.v. The emissivity for a 1 cm thick plane may be calculated directly from the absorption cross section. The density of O^- atoms (N_{O^-}) is given by F.R. Gilmore***; for 8000°K and .85 normal density it is $3.5 \times 10^{14}/\text{cm}^3$. The resulting emission is plotted in Fig. 1. The emissivity has been extrapolated linearly below 4000Å where there is no cross-section data. This extrapolation is not very serious since the N_2 and NO radiation become predominant in this region.

* W.R. Jarman and R.W. Nicholls, Can. J. of Phys, 32, 201 (1954) R.G. Turner and R.W. Nicholls, Can. J. of Phys, 32, 475 (1954).

** L.M. Branscomb and S.J. Smith. Phys Rev. 98, 1127 (1955).

*** F.R. Gilmore, Rand Corporation Research Memorandum, RM-1543 (1955).

The fraction of black body radiation accounted for by the free-bound transitions for a 1 cm layer of gas is about 0.4%. The major uncertainty in this result is in the validity of the cross section data. As Branscomb and Smith point out, there is an unresolved conflict between the ionization potential of O^- which they obtain (1.5 ev) and the one (2.2 ev) obtained by several previous experimenters using other experimental methods.

The radiation due to free-free transitions may be calculated very crudely on the basis of a hydrogen-like model. Using Kramer's absorption formula and integrating over a Maxwell-Boltzmann distribution of electron speeds, Unsold* derives the absorption coefficient.

$$\mu_{ff} = \frac{4\pi}{3\sqrt{3}} \frac{Z^2 e^6}{h c m^2 \sqrt{\pi k T / 2m}} \frac{1}{\nu^3} N_o N_e$$

where Z is the effective nuclear charge. Z may be determined by making the Bohr formula of the ionization potential give the value determined by Branscomb and Smith for O^-

$$\frac{Z^2 e^2}{2 a n^2} = 1.5 \text{ ev} \quad \rightarrow \quad Z = .66$$

$a n^2$ is the radius of the hydrogen Bohr orbit of principle quantum number n .

Quantum mechanical calculations by Hammerling and Kivel show that the absorption coefficient and hence the emissivity of this Bremsstrahlung is a factor 10 smaller than the above estimate. This calculation is based on measurements of the conductivity of high temperature air by Lamb and Lin. The radiation is small because the amplitudes of both s and p waves (0 and 1 unit of angular momentum) are small. Higher partial waves are kept out of the atomic field by their centrifugal potentials. Nitrogen is expected to be $1/2$ as effective as oxygen.

Consequently the emissivity sketched in Fig. 1 for O_{ff} which assumes $Z = .66$ is too large. It should be reduced by a factor like 5 to take account of both O and N free-free radiation. The emissivity at wave lengths less than 1μ is on the order of .1%.

ACKNOWLEDGEMENTS

The authors of this report wish to acknowledge the interest and support of all members of the Avco Research Laboratory throughout the course of the work. They are particularly indebted to Arthur R. Kantrowitz, Director of the Laboratory and Harry Petschek, for many stimulating discussions and critical reading of the final manuscript, Rochelle Prescott for design of the drum camera spectrograph and all other auxiliary optical apparatus, John C. Camm for assistance with the spectroscopic studies. Valuable contributions were also made by Avco consultants and friends, H. A. Bethe, G. H. Dieke, F. F. Marmo, H. L. Mayer, and R. Meyerott. Most of the data were accumulated by Richard M. Carbone, James B. Trask, Raymond Gardner, Weldon Nelson, and James E. Trider. Elmer J. Smith and Malcolm K. Hubbard assisted ably and efficiently in running the shock tube.

* A. Unsold, Physik der Sternatmosphären (Springer, Berlin, 1938) p. 117.

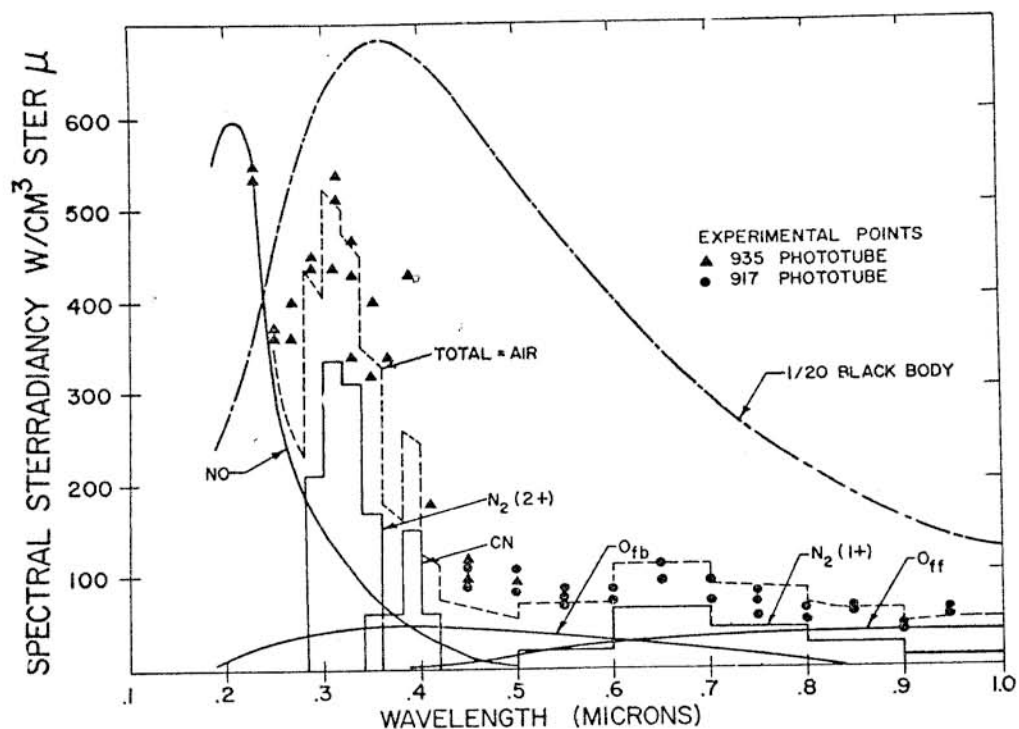


Fig. 1. Spectral sterradiancy of 1 cm of air at 8000°K and .85 normal density.

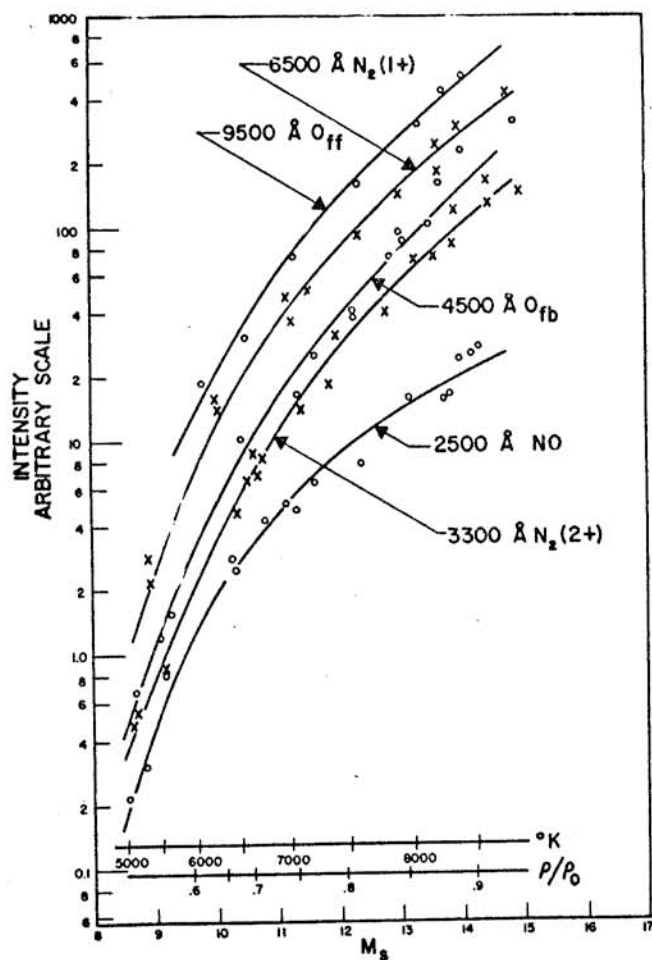


Fig. 2.
Radiation from air
vs.
Mach number.

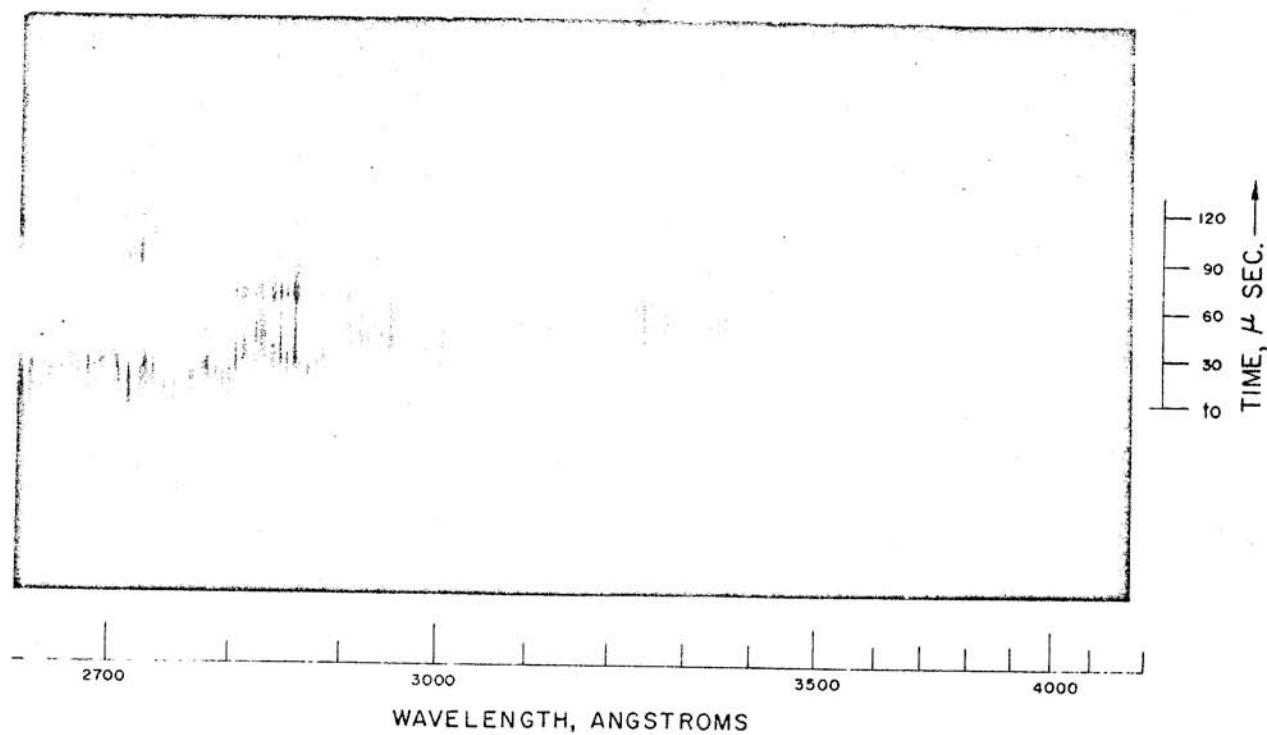


Fig. 5. Shock spectrum in air, 2600 to 4000^oA region (type 103-O film) $\rho = 1$ cm;
 $M_s = 14.1$; $T = 8400^{\circ}\text{K}$

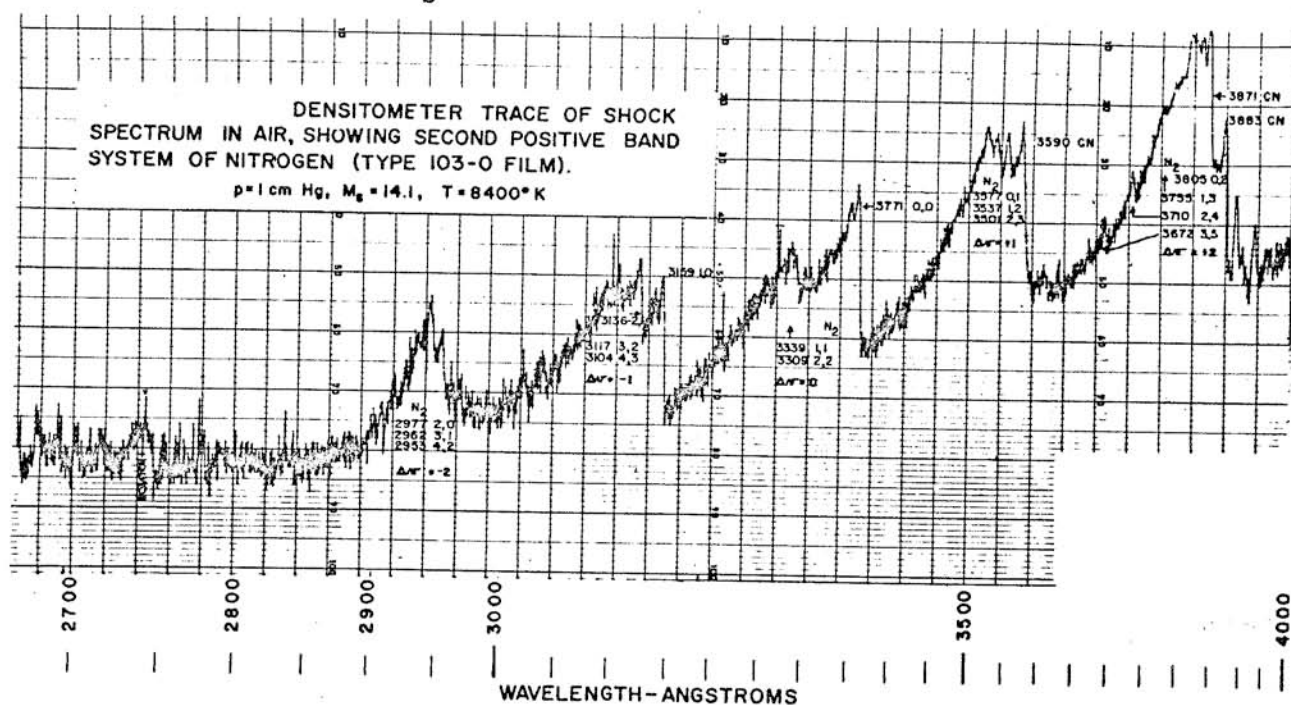


Fig. 6.

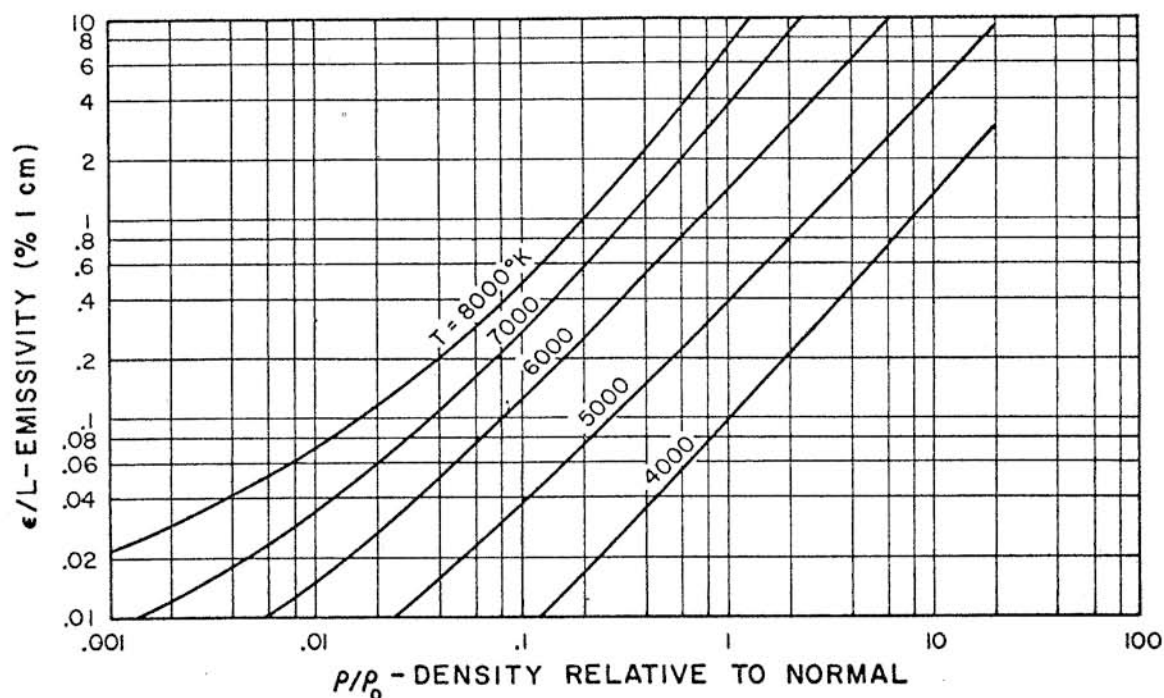


Fig. 3. Emissivity of 1 cm of air (valid for optically thin layers only)

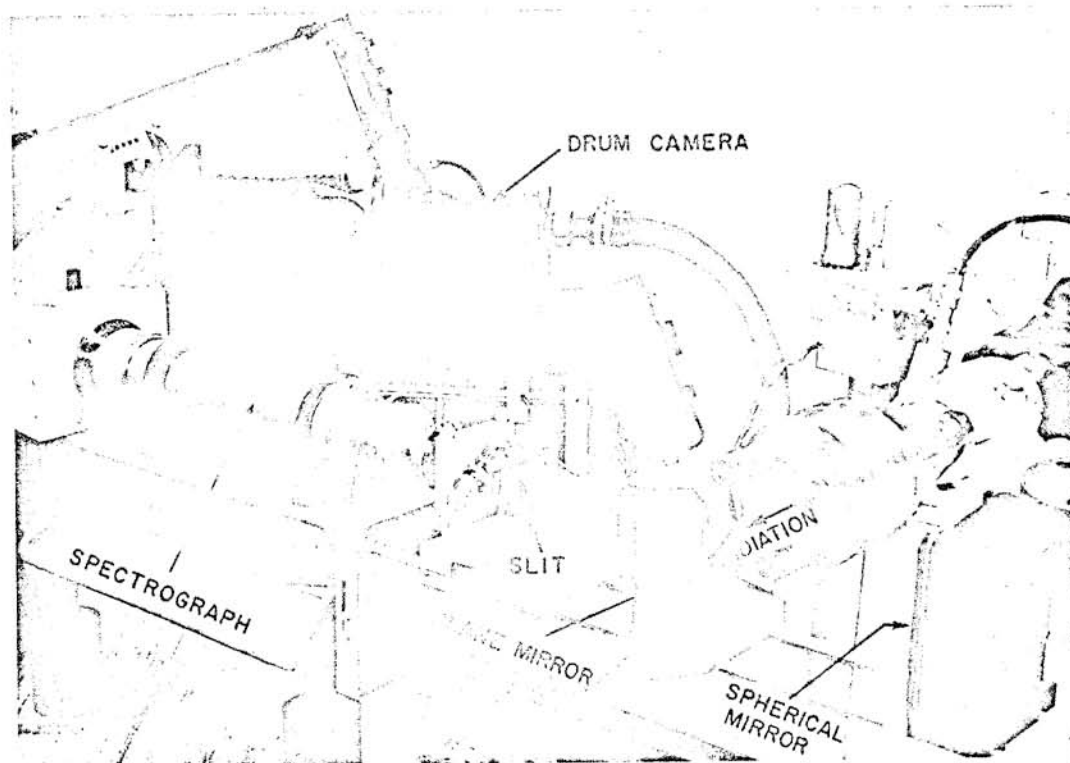


Fig. 4. DRUM-CAMERA RECORDING SPECTROGRAPH
The radiation passing through a quartz window at the end of the shock tube is reflected off a plane mirror onto a spherical mirror and imaged at the entrance slit of the spectrograph.

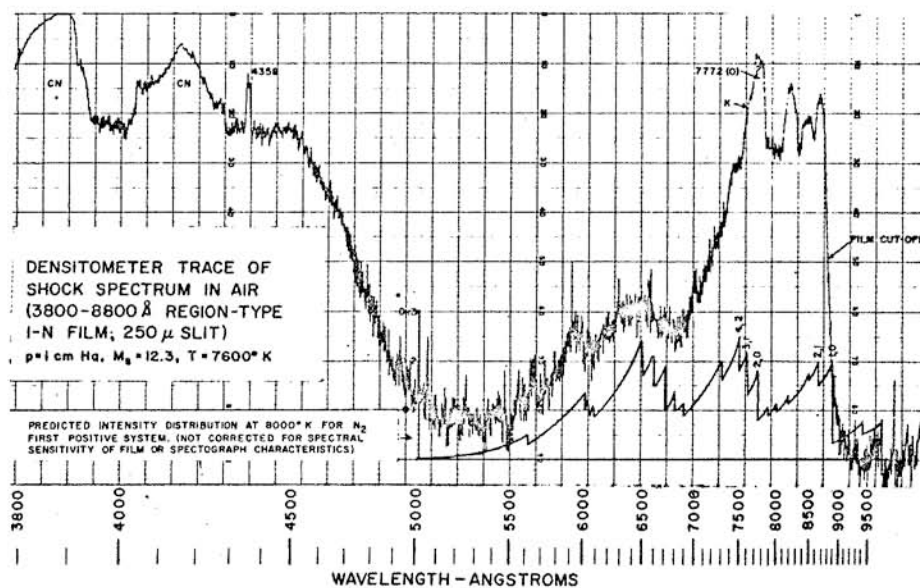
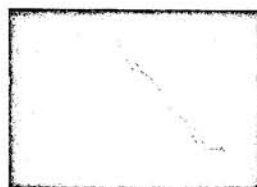
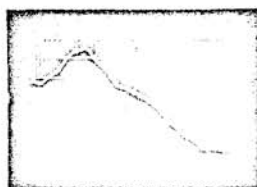
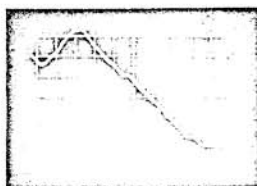


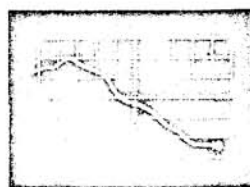
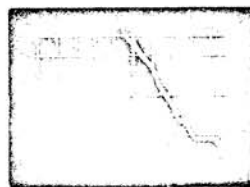
Fig. 7.

PHOTO TUBE TRACES OBTAINED WITH MONOCHROMETER

VIOLET SPECTRUM

 $\lambda = 3100 \text{ Å}$  $\lambda = 3500 \text{ Å}$  $\lambda = 3900 \text{ Å}$
 $\left| \begin{array}{c} 30 \mu \text{ SEC} \\ \text{TIME} \end{array} \right|$

RED SPECTRUM

 $\lambda = 5500 \text{ Å}$  $\lambda = 6500 \text{ Å}$  $\lambda = 7500 \text{ Å}$
 $\left| \begin{array}{c} 30 \mu \text{ SEC} \\ \text{TIME} \end{array} \right|$

SWEEP SPEED = 5 $\mu\text{s}/\text{cm}$
 TEMPERATURE $\sim 8,000^\circ \text{K}$
 DENSITY $\sim .85 \text{ ATMOSPHERIC}$

Fig. 8.